Article

Optimization of human cancer cell xenograft into zebrafish larvae for anti-cancer drug screening

Meghan G. Haney [1,2], Lyndsay E.A. Young [1], L. Henry Moore [1], Yelena Chernyavskaya [1], Min Wei [3], Kia H. Markussen [1], Alyse Ptacek [1], Stephen Dockins [4], William C. Sanders [1], Ramon C. Sun [2,5]*, and Jessica S. Blackburn [1,2]*

[1] University of Kentucky, College of Medicine, Department of Molecular and Cellular Biochemistry
[2] University of Kentucky, Markey Cancer Center
[3] Guangdong Pharmaceutical University
[4] Ohio University, Heritage College of Osteopathic Medicine
[5] University of Kentucky, College of Medicine, Department of Neuroscience
* Correspondence: ramon.sun@uky.edu (RCS), jsblackburn@uky.edu (JSB)

Abstract: Transplant of human cancer cells into zebrafish larvae has emerged as a useful methodology in cancer research. Zebrafish have very low husbandry costs, are amenable to large-scale drug screening, and are unmatched for optical clarity in live animal imaging. However, there is currently no consensus on the ideal methods for xenograft of human cancer cells into zebrafish. Here, we have examined the effects of transplant site and housing temperature on both zebrafish larvae and human cancer cells using survival analyses, metabolomic approaches, and *in vivo* imaging. Our data show that while zebrafish larvae can adapt to the ideal conditions for mammalian cells, human cancer cells are highly sensitive to both temperature change and transplant site. Human cells housed in slightly cooler than physiologic temperatures had a significantly altered metabolism that resulted in changes in growth, survival, and response to chemotherapy. Cancer cells xenografted into the yolk of the larvae also had reduced proliferation and drug response compared to those xenografted into the soma, in part due to the differences in metabolites available at these sites. In total, temperature and transplant site can have profound effects on xenografted cells. Standardization of zebrafish xenograft methods will enhance data reproducibility between individual laboratories.

Keywords: *gas chromatography mass spectrometry, metabolomics, acute lymphoblastic leukemia, confocal microscopy, high-throughput drug screens, VAST*

Graphical Abstract:

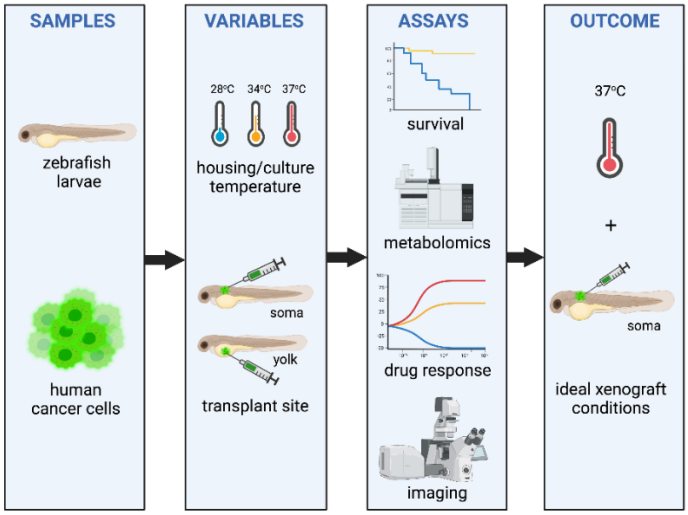

1. Introduction

Xenograft of human cancer cell lines and primary patient derived tumor cells into research animals is a widespread practice, particularly for validating response of tumor cells to novel drug therapies within the context of a whole organism. Historically, immune compromised mice have been the most common recipient of human cell xenografts. Over the last decade, zebrafish have risen in prominence for their use in transgenic models of human cancers, and in recent years, researchers have shown that zebrafish are also a useful complement to the mouse in the xenograft setting [1-7].

Compared to mice, zebrafish are incredibly cost-effective due to their large brood size, quick generation time, and inexpensive husbandry needs. For these reasons, zebrafish larvae have been used with great success in large-scale drug screens to identify novel small molecules that regulate developmental and disease processes in humans. Drugs can be dissolved in aqueous media and administered to larval zebrafish in 96-well plates. Animals will absorb the drug through their skin, reducing drug usage and eliminating the need for tedious animal injections [4,8]. Additionally, some zebrafish strains have been engineered to lack pigment [9], allowing for *in vivo* high-resolution imaging of tissues and organs that are otherwise inaccessible in mouse. Finally, zebrafish do not develop a fully functional immune system until 7 days post-fertilization (dpf), which allows for the use of wild-type zebrafish in engraftment experiments without the need to generate immune-compromised animals via irradiation or genetic manipulation [10]. Given these advantages of zebrafish in research, human cancer xenograft was a logical next step forward with this model.

The first use of human cell xenograft in zebrafish was reported in 2005, when green fluorescent protein (GFP)-labeled human cell lines were transplanted into blastula stage embryos [11,12]. Since then, several groups have published various methods for xenografting human cell lines and primary patient- or mouse-derived tumor cells into zebrafish, from embryos to adult animals [2,3,6,7,11,13,14]. Recently, humanized zebrafish were even developed to express human cytokines to help facilitate xenograft engraftment [15]. Researchers have also postulated that zebrafish xenografts could play a new and important role in personalized medicine—thousands of zebrafish could be transplanted with a patient's tumor, and a drug screen could quickly identify which chemotherapies the tumor is most susceptible to, and this information could be used to help inform patient treatment [3,14]. This excitement stems from the major benefit of zebrafish over mouse xenografts, which is their amenability to drug screening. Following xenograft, larvae can be housed in 96-well plates containing drug, and both the toxicity of the drug to the animal and the response of the cancer cells to the drug can be simultaneously assessed. Methods to quantify the drug response in zebrafish xenograft currently vary from dissociation of xenografted fish into single cell

suspensions and quantification of remaining, fluorescently-labeled tumor cells [16,17] to semi-automated imaging methods of both fish and engrafted tumor cells [18-21].

Despite the many advantages of zebrafish as a xenograft model, some concerns remain. Pharmacokinetic and pharmacodynamic studies examining the absorption and metabolism of drugs administered to zebrafish larvae through aqueous media are sparse [22-24]. It is unclear how much of the drug that is dosed into the media actually targets the tumor cells, which can lead to false negatives in drug screens. Also, the development of the zebrafish adaptive immune system after 14 days of life will lead to tumor rejection and prevents researchers from assessing the development of tumor drug resistance and tumor recurrence, which are major issues in the cancer clinic [10]. While immune-compromised adult zebrafish have partially met this need, adult immunodeficient zebrafish must be injected or undergo oral gavage to deliver drug so are not as amenable to large-scale drug screening [13].

Whether the fish used in xenograft are larvae or immunocompromised adults, there are several inconsistencies in xenograft methods that should be resolved, including the transplantation site used for xenograft and the housing temperature that xenografted animals are held at. Ultimately, a lack of consensus in the field can lead to challenges in replicating data between research groups and prevent widespread use of zebrafish xenograft assays in cancer research. For example, xenograft of cells into the yolk of larva is common practice because it can be done very rapidly and with high survivability by the animal—this technique places human cells in an acellular, lipid-rich microenvironment [25-28]. It is not clear if human cells would survive differently if transplanted into the yolk versus xenograft into zebrafish somatic tissues, which is a method published by several other groups [29-31]. Drugs likely also absorb much differently into the yolk compared to the body of the zebrafish, which could lead to inconsistencies in how xenografted cells respond to drug treatment [24].

Temperature differences are also a major concern. Zebrafish are normally housed at 28°C, much cooler than the 37°C body temperature of humans and other mammalian model organisms. As a compromise, xenografted fish are routinely kept at 34°C to try to maintain both zebrafish and human cell survival; however, this temperature change likely affects both normal zebrafish and cancer cell physiology [32,33]. For example, increasing the temperature that zebrafish are maintained at can increase the accumulation of chemicals from media into zebrafish tissues, leading to enhanced chemical toxicity in fish [34,35] . Temperature also has a significant impact on the growth and development of zebrafish larva, which could affect the tumor microenvironment of xenografted cells [36,37]. Acclimation of zebrafish to warm temperatures also depletes their energy stores and can change levels of enzymes involved in metabolic processes such as energy metabolism and oxidative phosphorylation [36,38]. It is unclear how these changes to the host might ultimately affect the survival of the xenografted cells or their response to drug treatment.

Overall, a more complete understanding of the effects of human cell xenograft in zebrafish, both to the human cells being transplanted and to the recipient zebrafish themselves, is needed as zebrafish xenografts become more widely used. Here, we have examined thousands of xenografted larvae and completed metabolic profiling to delineate the effects of xenograft transplantation site and animal housing temperature in zebrafish xenograft models. We have found that these variables significantly influence both zebrafish and human cell survival and metabolism. However, warmer temperatures of 34°C and 37°C are less detrimental to zebrafish than the cooler temperatures to human cancer cells, which do not respond as well to chemotherapy after xenograft when housed at 34°C. Cells xenografted into the yolk of zebrafish larvae also had marked differences in proliferative capacity and drug response, compared to cells transplanted into somatic tissues. In total, our findings highlight some considerations that should be made in the experimental design of zebrafish xenograft to ensure that useful and reproducible data is generated from these types of assays.

2. Results

2.1. Recipient zebrafish survival post-xenograft varies by transplant site

Common variables in zebrafish xenograft studies are the site of mammalian cell transplantion and number of cells injected per animal. Given that most downstream applications of zebrafish xenografts involve drug screening, it is important to achieve reliable engraftment of human cells in the fish while still maintaining high survival rates of the animal. To determine an optimal engrafment site, we stained a panel of human cancer cells, including leukemia, glioblastoma, colorectal, breast, and lung cancer cells with DiI (a fluorescent, lipophilic, cationic dye) and injected 500 cells into dechorionated zebrafish larvae at 48 hpf at 7 different injection sites: yolk, pericardial space, brain, caudal vein, duct of Cuvier, periorbital space, and perivitelline space (**Figure 1A**). Xenografted animals recovered from the procedure at 28°C, then were transferred to 34°C. The cell number and housing conditions are commonly used in zebrafish xenograft [33]. Overall, we examined at least 450 xenografted animals for each transplant site, for a total of >3,150 larvae used in these experiments. There was no major difference in animal survival based on the human cancer cell type transplanted or the transplant site at 1 day post transplant (dpt), with an average of 85% percent of zebrafish surviving the xenograft procedure (**Figure 1B, Supplemental Table 1**). The number of surviving fish that also engrafted the xenograft did vary slightly but not significantly between the transplant sites, averaging 77%. In all cases, once engraftment was observed at 1 dpt, engraftment was maintained in the animals for up to 5 dpt. Longer timepoints were not assessed due to emergence of the host immune system. However, in every xenograft site examined, and with every cancer cell type tested, there was a signficant decline in zebrafish survival between 1 and 5 dpt, in some cases dropping by as much as 35% (**Figure 1C**). We found that the pericardium, duct of Cuvier, and yolk injection sites provided the most reliable results with the highest percentage of engrafted fish still alive at 5 dpt. Another important consideration for use of xenograft in high-throughput studies is ease of injection—caudal vein and retro-orbital transplants took approximately twice as long as other injection sites due to the preciseness needed to puncture these veins (**Supplemental Table 1**). Cancer cells were also routinely seen circulating after transplant into the caudal vein, duct of Cuvier, peri-orbital space, pericardial space, or perivitelline space. Overall, we found that transplant into the yolk and pericardial space provided the most consistent results in zebrafish engraftment, survival, and cell placement; these sites were chosen going forward for further studies.

A common critique of xenograft into larval zebrafish is that transplant with low cell number will reduce the effects of tumor heterogenity in the downstream analyses [2]. We next compared the practicality of a transplant cell density of 100, 250, 500, and 1,000 cells per zebrafish larvae both in the yolk and in pericardial space of the fish. We were able to see consistent engraftment of the cells at 1 dpi in the yolk with 100 cells injected, but were unable to reliably visualize and quantify engrafted cells when less then 500 cells were injected in the pericardial space (**Figure 1D-E**). We also found there to be a significant reduction in survival in animals tranplanted with 1,000 cells in the yolk (p=0.0396), although larvae injected in the pericardial space surived equally well at any transplant cell number (**Figure 1F-G**). Together, these data show that zebrafish are able to tolerate xenograft of a wide range of cancer cell types, tranplantation sites, and cell numbers. The

spontanous and significant decline in surivial between 1 dpt and 5 dpt is also important to note, as this will affect the numbers of engrafted animals that are needed per experiment.

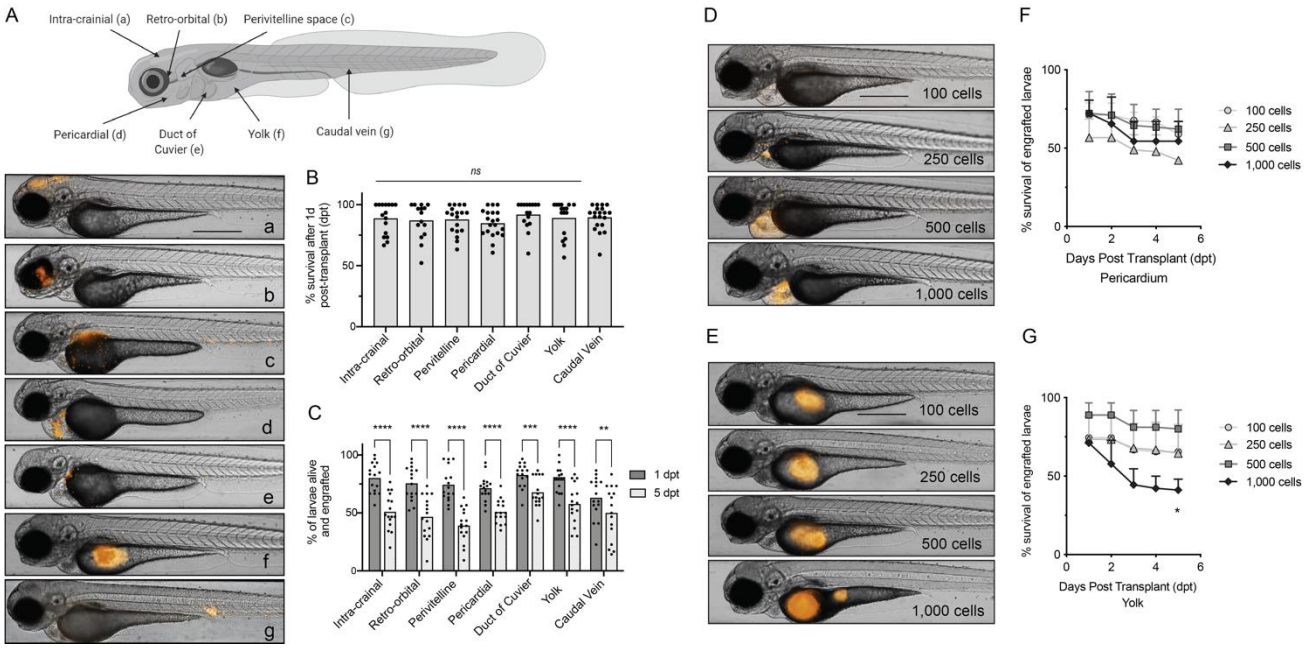

Figure 1. Zebrafish larvae are amenable to xenograft at mulitple site and cell doses, although survival decreases over time. (**A**) Depiction of seven injection sites tested in 48 hour post-fertilization (hpf) larvae: intracranial (a), retro-orbital (b), perivitelline space (c), pericardium (d), duct of Cuvier (e), yolk (f), and caudal vein (g). Representative images are of larvae at 1 day post-transplant (dpt) with DiI stained human cancer cell lines. (**B**) Percent survival of xenografted fish after 1dpt at the indicated transplantation site. Bars show the average percent survival, and each data point represents 30 xenografted larvae. (**C**) Comparison of percent survival of engrafted larvae after 1 and 5 dpt at the indicated transplantation site. Each data point represents 30 xenografted larvae, and the bars are the average of each group. (**D**) The indicated doses of the DiI stained, human Jurkat human leukemia line were transplanted into the pericardial space and (**E**) yolk of 48 hpf zebrafish. Daily survival rates were recorded each day for 5 days for (**F**) pericardium and (**G**) yolk xenografted larvae. Each data point represents 3 clutches of 30 xenografted zebrafish each, at 0 dpt. Error bars are the standard deviation. Ns, not significant, *p<0.05, **p<0.01, ***p<0.001, ****p<0.0001. Scale bars in images represent 250 µm.

2.2 Increases in housing temperature alter zebrafish survival and metabolism

A challenge in zebrafish xenograft experiments is the large temperature difference between the optimal growth conditions for zebrafish larvae versus human cancer cells. Zebrafish are normally housed at 28°C while mammalian body temperature is 37°C. There is inconsistency in zebrafish xenograft methods, with researchers using a range of temperatures between 28°C and 37°C for maintenance of zebrafish after xenograft [32,33]. To asses the effects of increased housing temperature on larval survival, we examined the survival of >250 Casper, AB, and SAT strain zebrafish larvae over three different temperatures. As expected, survival was highest at 28°C with 95% of animals surviving to 5 days, while the survival rates at 34°C and 37°C was 80% and 67% respectively (**Figure 2A**, **Supplemental Table 1**). Gross morphologic changes were noted in the zebrafish when the temperature increased from 28°C to 34°C and 37°C, with the size of the yolk sac decreasing with increasing temperature and the fish appearing smaller in size and less active at higher temperatures (**Figure 2B**). Survial rates were similar across all strains. We also compared survival of xenografted fish that were injected with different human leukemia cell lines in either the pericardial space or yolk and housed at 34°C or 37°C. Zebrafish that were housed at 34°C had a survival rate after engraftment of cells of 73.45% ±9.26%, compared to 56.67% ±11.52% of larvae surviving when housed at 37°C (**Supplemental Table 2**). Xenografts into the pericardium also tended to have higher survival than the yolk, with less variation between replicates.

A decreased yolk and smaller body size indicates potentially high energy expendatures in the fish housed in warmer temperatures. We examined the effects on temperature on metabolism of the

whole animal using gas-chromotography mass spectrometry (GC-MS) on tissues from larvae that had been housed for 48hr in 28°C, 34°C, or 37°C. In general, carbohydrate and amino acid levels increased when the temperatures were rasied from 28°C to 34°C. (**Figure 2C-D and Supplemental Table 3**). Interestingly, we did not see additional metabolic increases in animals as the housing temperature increased from 34°C to 37°C (**Figure 2C-D**); the levels of some metabolites were slightly decreased comparing those animals at 34°C versus 37°C (**Supplemental Table 3**). The general upward trend of most metabolites may be indiciative of changes in the unfolded protein repsonse (UPR), which occurs cells undergoing stress such as a heat shock [39,40]. The UPR is involved in crucial steps in lipid, glucose, and protein metabolism and our data show that general metabolic processes in larvae are increased when housing temperatures are raised from 28°C to 34°C. The subsequent decrease in free metabolites when larvae are further heated to 37°C may represent zebrafish cells entering a salvage mode due to increasing stress from the higher temperature. As a whole, these data highlight that variations in temperature can signficantly change the metabolism of the entire zebrafish, which in turn may impact the nutrient availability and microenvironment of the xenografted cells.

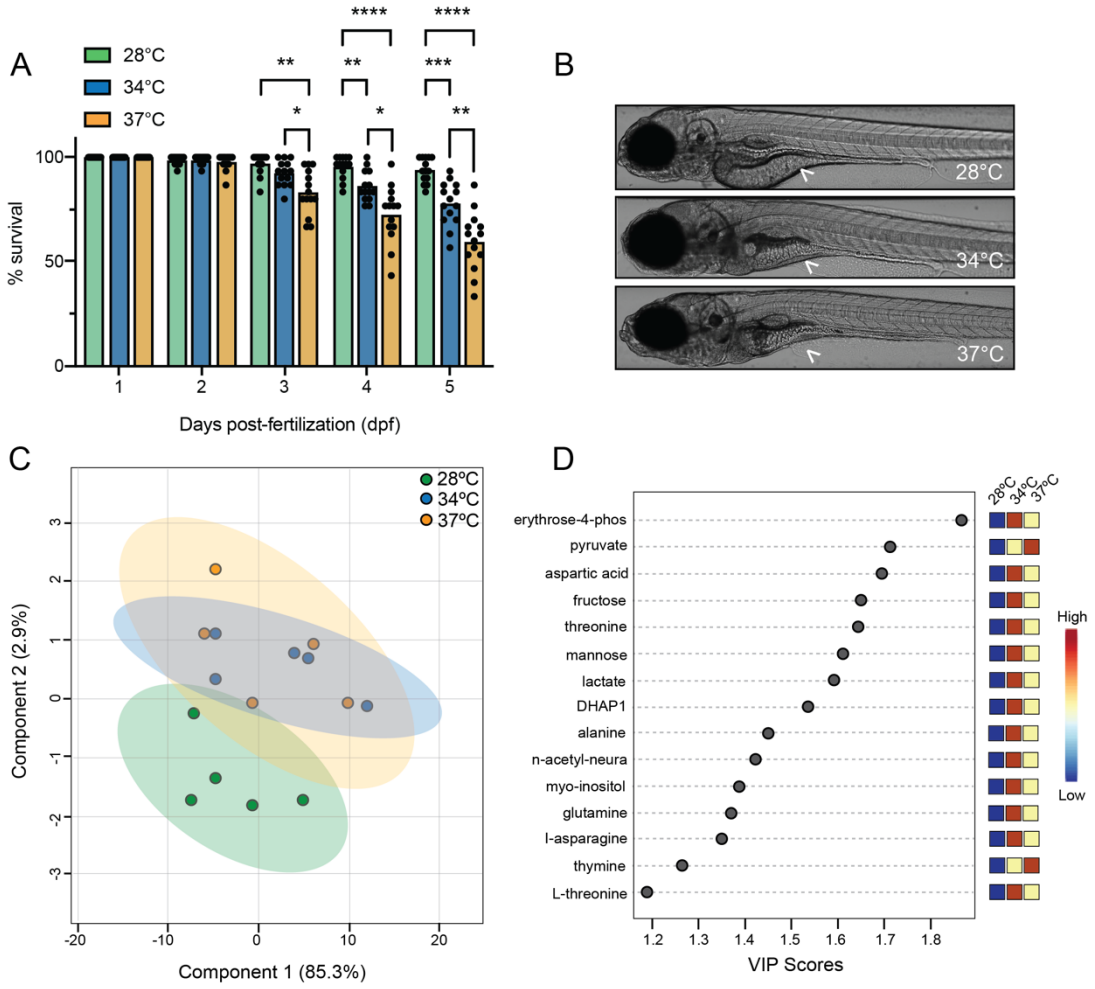

Figure 2. Housing temperatures of 34°C and 37°C similarly impact zebrafish survival and metabolism. (**A**) Survival of zebrafish larvae at 28°C, 34°C, and 37°C. Fish were dechorionated at 48 hpf and incubated at the designated temperature for 5 days. Plots show the average surviving larvae at each temperature and time point. Data points are individual clutches of 30 larvae. *p<0.05, **p<0.01, ***p<0.001, ****p<0.0001. (**B**) Representative images of 7 dpf zebrafish after housing at 28°C, 34°C, and 37°C for 5 days. Arrowhead is in the same location in each image to highlight decreasing yolk size at increasing temperature. (**C**) Partial least squares discriminate analysis (PLS-DA) shows larvae housed at 28°C have different metabolic profiles than those housed at 34°C or 37°C. (**D**) Indicates the selected metabolite/variable's importance in the PLS-DA model. Metabolites involved in carbohydrate and amino acid metabolism are shown.

2.4 Decreases in cell culture temperature alters human cancer cell survival, metabolism, and response to chemotherapy

Next, we examined the effects of temperature on human cancer cells. The human T-cell Acute Lymphoblastic Leukemia (T-ALL) cells that we used in this study did not proliferate at 28°C, so we only assessed the effect on maintaining cells at 34°C versus the physiological 37°C. We found that all cell lines were able to proliferate 34°C over a period of 5 days, but the rate of proliferation was significantly slower at 34°C compared to 37°C (**Figure 3A**). This growth change was likely assoicated with fewer cells actively replicating in S phase at 34°C, measured by EDU cell cycle analysis (**Figure 3B**). Interestingly, we saw an approximate 2-fold increase in apoptosis of two leukemia cell lines when maintained at 34°C compared to 37°C, quantified by Annexin V staining, but one cell line had no change in apoptosis rate (**Figure 3C**). These data suggest that not all cell lines respond in the same way to lower growth temperatures.

Next, we evaluated changes in overall metabalic activity under growth at cooler temperatures. Jurkat cells were cultured at 34°C and 37°C for 24 hr and analyzed by GC-MS. We observed that many metaoblites involved in engery metabolism where changed when cells were cultured at 34°C (**Supplemental Table 4**). For example, metabolites associated with the TCA cycle, the main source of energy for the cell, were increased when cells were cultured at 34°C (**Figure 3D and 3F**), indicating that the cells housed in cooler temperatures were producing more ATP. Seahorse analysis of mitochondiral bioenergeitcs also showed that ATP production rates and coupling efficiency were signficantly increased in human cell lines grown at 34°C compared 37°C (**Figure 3G and 3H**). Mammalian cells often produce ATP during in response to cold, and these data suggest that cells cultured at 34°C may be undergoing a thermogeneic reponse [41]. This change in metabolic function at 34°C might impact cancer cell behavior and drug responsiveness in zebrafish xenograft experiments.

Figure 3. A lower culture temperature of 34°C impact human cancer cell metabolism and viability. (**A**) Viable cell counts of three human T-cell acute lymphoblastic leukemia cell lines (Jurkat, HPB-ALL, and HSB2) at 34°C (blue) and 37°C (orange). Data represent an average of 3 biological replicates with at least n=3 technical replicates per experiment. (**B**) Percent of Jurkat cells in each phase of the cell cycle, determined by EdU uptake at 34°C and 37°C. (**C**) Percent apoptosis in three human leukemia lines determined by Annexin V staining at 34°C and 37°C. Data for EdU and Annexin staining represents an average of n=3 replicates per temperature, and standard deviation is shown. (**D**) Schematic of the Krebs cycle. (**E**) VIP plot showing the relative importance of each Krebs cycle related metabolite in the PSL-DA model show in (**F**). The PSL-DA analysis shows that Jurkat cells grown at 34°C cluster independently than those grown at 37°C, based on the metabolites present in the cells. Seahorse analysis performed on Jurkat and HSB2 cells shows an increase in ATP production rate (**G**) and coupling efficiency (**H**) at 34°C compared to 37°C. Data represents an average of 10 replicates per group with error bars representing standard deviation. For all, *p<0.05, **p<0.01, ***p<0.001, ****p<0.0001.

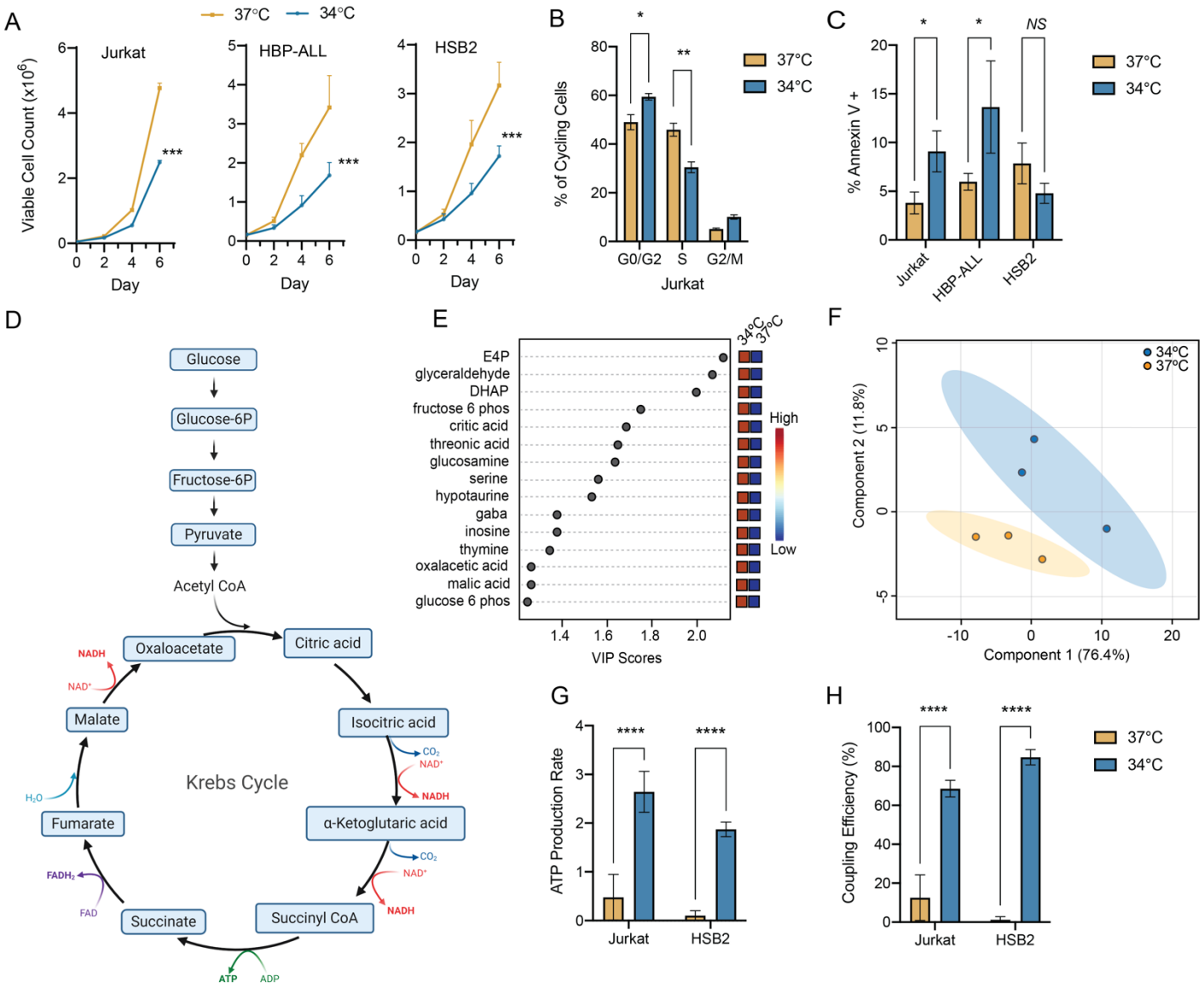

The metabolic activity of cancer cells plays an important role in how the cells respond to drug treatment [42,43]. We treated human T-ALL cell lines with chemotherapies commonly used to treat T-ALL in clinic (Cytarabine, Dexamethasone, Methotrexate or Vincristine). Cells were treated for 72 hours at 34°C and 37°C. We found that drug response varied based on cell line and temperature. For example, Jurkat cells are resistant to the glucocorticoid Dexamethasone [44]—this resistance was more pronounced with treatment at 37°C (p<0.01, **Figure 4A**), likely because the cells are more actively proliferating at their physiologic temperature (**Figure 3A**). While temperature had no significant effect on Jurkat response to Cytarabine and Vincristine, cells were resistant to Methotrexate at 34°C but were readily killed at 37°C (p<0.0001, **Figure 4A**). Methotrexate prevents synthesis of tetrahydrofolate, which in turn is necessary for the generation of nucleotides used in DNA synthesis and cell division. Reduced activity of the folate synthesis pathway at 34°C may impact how readily the cells respond to Methotrexate treatment. Interestingly, temperature had no impact on chemotherapy treatment in the HSB2 T-ALL cell line, with no significant difference in any dose response curve (**Figure 4B**). Together, these data highlight the impact that changes in temperature can have on cancer cell metabolism and subsequent response to drug. These data also show that these effects are also not easy to predict. Cancers are heterogeneous and changes in temperature will affect their metabolic pathways and drug responses differently, within the same cancer type and likely even within the same tumor sample.

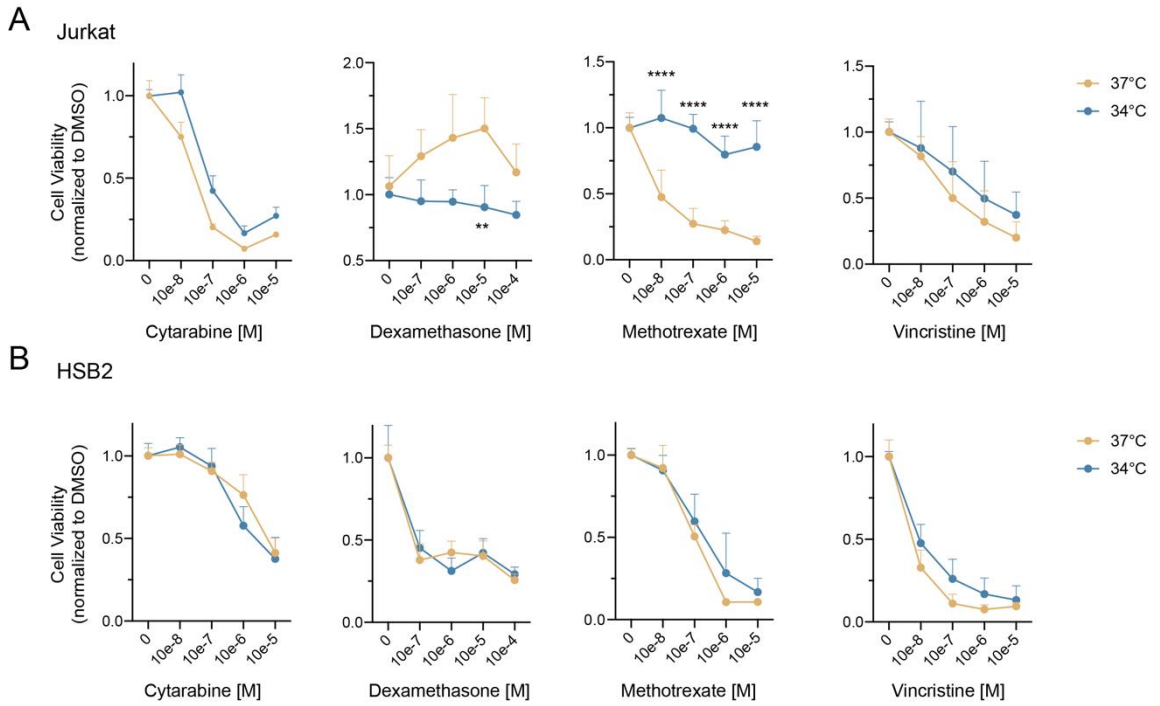

Figure 4. Human cancer cell lines can respond to chemotherapy differently based on temperature. (**A**) Jurkat and (**B**) HSB2 human T-cell acute lymphoblastic leukemia cell lines were cultured at 34°C (blue) and 37°C (orange) and treated with increasing concentrations of the following drugs: Cytarabine, Dexamethasone, Methotrexate, or Vincristine, as indicated. Cell viability was measured by CellTiter-Glo after 72 hours of drug treatment and normalized to DMSO vehicle control. Error bars represent standard deviation. **p<0.01, ****p<0.0001.

2.5 DiI membrane-labeling fluorescent dyes may not be suitable for longer-term xenograft assays

Human cells are typically stained with membrane-labeling fluorescent dyes, such as Vybrant DiI Cell-Labeling Solution, so they can be easily visualized after xenograft into zebrafish. Although these protocols are well established [16,25,45] and we sucessfully used these methods to monitor well-injected and engrafted larvae (**Figure 1**), at later time points and upon examination with confocal microscopy, we observed that staining had became punctate, and many cells lost DiI labeling completely (**Figure 5A**). This latter effect may be due to the nature of the dye—DiI stains the membrane and the stain will be diluted in subsequent generations of cells as they proliferate. However, the brighter punctate DiI staining was difficult to differentiate as either part of an intact cell or cell debris (**Figure 5A**), which may lead to difficulties in assessing cancer cell response to drug. *In vitro,* DiI staining of cells had no immediate impact on cell proliferation or apoptosis, measured by EDU and AnnexinV repsectively (**Supplemental Figure 1**). However, we found that DiI stained cells did not incorperate BrdU *in vivo* (**Figure 5A**). It was not clear whether the DiI stained cells were not proliferating *in vivo*, or if DiI labeling somehow prevented BrdU uptake or visualization. Overall, our observations are in line with others who have recently shown that DiI stained cells do not survive well after zebrafish xenograft [7]. Given the unexpected appearance and behavior of DiI stained cells in zebrafish xenografts, we used human T-ALL cell lines that stably expressed GFP for subsequent studies.

2.6 Transplant site strongly impacts the growth of human cancer cells in zebrafish

To determine the extent to which transplant site and housing temperature afftects xenografted cells *in vivo*, we xenografted GFP-expressing human T-ALL cell lines (Jurkat or HSB2) into either the pericardial space or yolk of zebrafish larvae. Zebrafish were housed at 34°C or 37°C for 48 hr and underwent BrdU and TUNEL staining to quantify the cellular proliferation and apoptosis, respectively, of engrafted cells. Surprisingly, housing temperature did not significantly affect the percentage of cells proliferating in either cell line. However, we found that while an average of 50%

of xenografted cells were actively proliferating at both 34°C and 37°C when transplanted into the pericardial space, we were unable to identify any BrdU-positive, activly dividing human cancer cells after transplant into the yolk (**Figure 5B-C**). Cells xenografted into the yolk were also not undergoing apoptosis, although there was significantly more apoptotic Jurkat cells xenografted into the pericardial space of larvae housed at 34°C, compared to 37°C (p=0.042, **Figure 5D-E**). Overall, these data show that the site of transplant in zebrafish xenogrant has a greater impact human cancer cell physiology, compared to housing temperature, with cells transplanted into th e yolk appearing more static than those transplanted to the zebrafish soma.

Figure 5. Xenografted human cancer cell growth is affected by injection site and temperature. Larvae xenografted with DiI stained Jurkat cells in either the pericardium or yolk were treated with BrdU for 24 hours. (**A**) are representative images showing DiI staining is faint and punctate in the cells, and BrdU/Alexafluor 488 staining is not present in the xenografted cells. (**B**) Representative images of Jurkat and HSB2 cells stably expressing *PGK:GFP* and xenografted into the pericardium or yolk of larvae, then housed at the indicated temperature. Larvae were treated with BrdU for 24 hours to label proliferating cells, and stained with anti-BrdU Alexafluor 555. (**C**) Quantification of the percent of BrdU-positive and GFP-positive xenografted cells in the pericardium or yolk at 34°C (blue) and 37°C (orange), showing significant proliferation in the cells xenografted into the pericardium and almost none in yolk injected cells. (**D**) Larvae were fixed 24 hours post-xenograft and stained with TUNEL to quantify apoptosis in GFP-positive Jurkat and HSB2 cells. (**E**) Quantification of the percent of TUNEL positive xenografted cells in the pericardium or yolk at 34°C (blue) and 37°C (orange), showing significant changes in apoptosis in cell lines based on temperature and transplant site. For all, nuclei were stained with Hoechst *p<0.05, **p<0.01, ***p<0.001, ****p<0.0001.

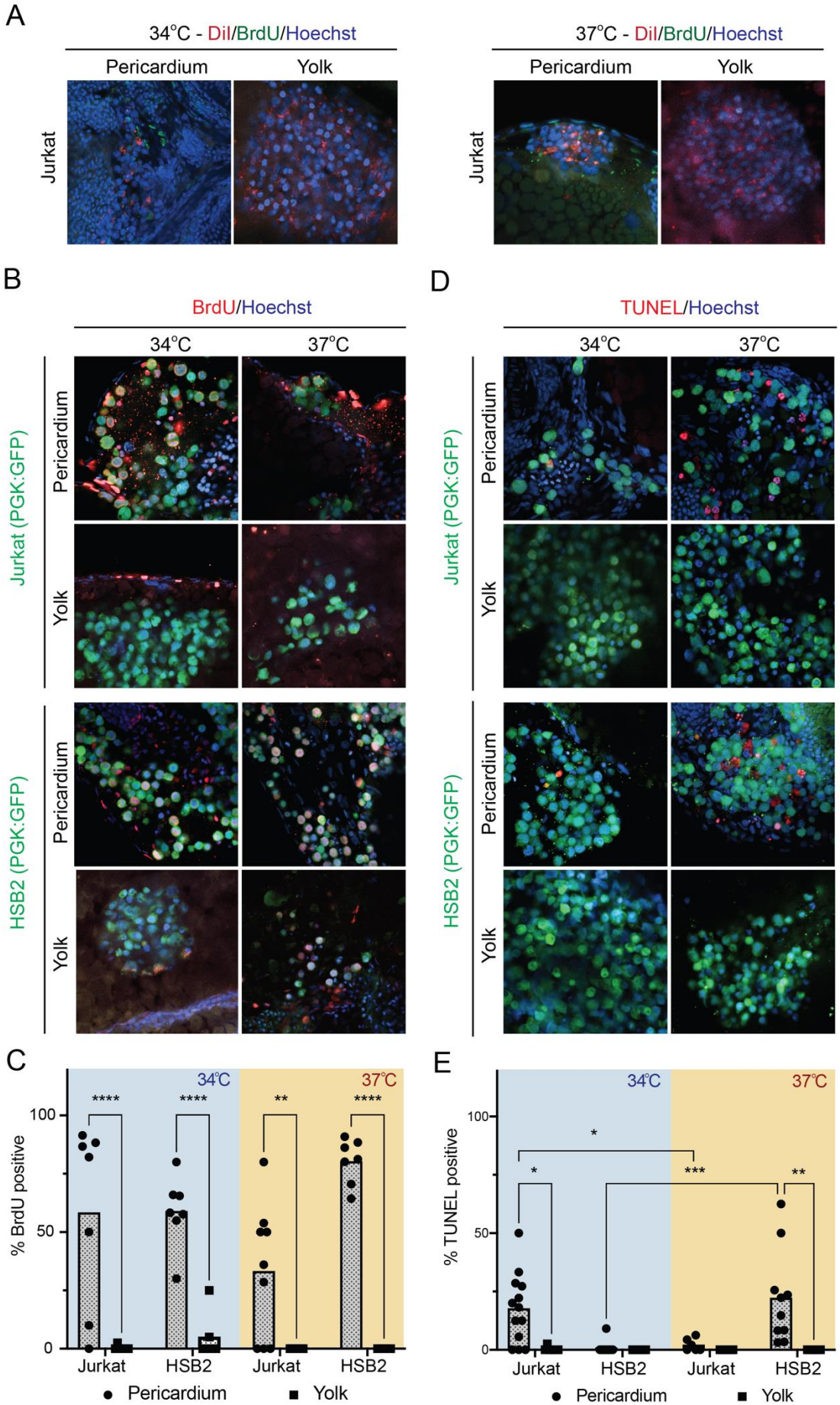

2.2 Metabolic differences between the soma and yolk may affect xenografted cells.

The zebrafish yolk is devoid of cells and largely made up of stored lipids and proteins that larvae feed off exclusively until 5-7 days of life [46]. This area is also the most common transplant site for xenograft models in zebrafish because it is both nutrient-rich and straightforward to inject into. However, we found that xenografted cells appeared senesced in the yolk—neither proliferating nor undergoing apoptosis. Since the yolk composition differs so markedly compared to the soma, it may have different metabolic activity that can impact the behavior of xenografted cells. To examine the metabolites present in the zebrafish yolk, zebrafish were either left intact or manually de-yolked at 5 dpf and metabolites were analyzed by GC-MS (**Figure 6A**). Fatty acids, amino acids, and sugars were enriched in the yolk (**Supplemental Table 5**). PCA analysis of metabolites linked with glycolysis showed that intact larvae with yolk clustered independently from de-yolked zebrafish (**Figure 6B-C**), indicating clear metabolic differences between soma and yolk. While metabolites appear readily available in the zebrafish yolk, the yolk is also highly viscous. The osmotic gradient needed for cells to take up glucose and other metabolites may be altered to such an extent in the yolk that the available metabolites simply cannot enter the cell. Human cells xenografted into zebrafish are already in a profoundly different microenvironment, and the composition of the yolk adds another layer of complexity that should be carefully considered when planning zebrafish xenograft experiments.

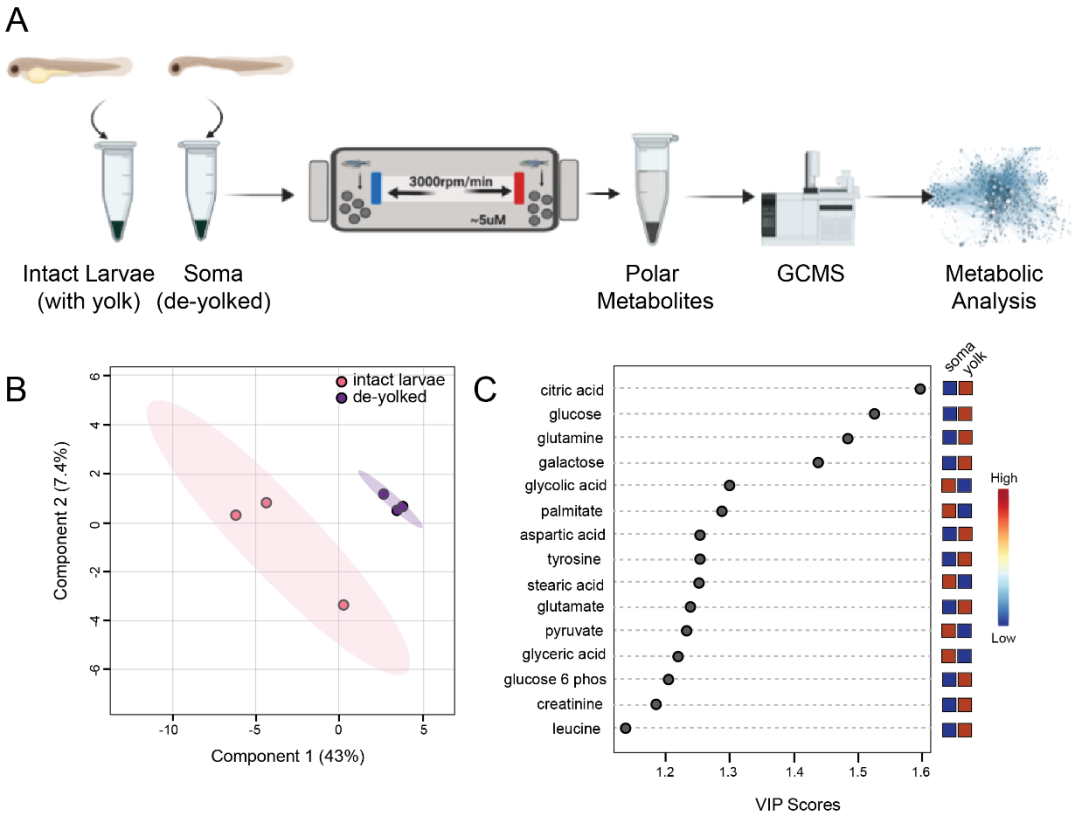

Figure 6. The available metabolites vary between the soma and the yolk of zebrafish larvae. (**A**) Schematic of the workflow for GC-MS metabolic analysis of whole zebrafish larvae and de-yolked zebrafish larvae. (**B**) Principal component analysis (PCA) showing intact zebrafish larvae (pink) cluster independently from zebrafish soma samples (purple), based on metabolites present in the samples. (**C**) VIP plot highlighting metabolites involved in energy production.

2.7 Both temperature and transplant site affect human cell response to drug treatment after zebrafish xenograft.

One major benefit of zebrafish xenograft is the ability to use xenografted larvae in high-throughput drug screening. Small molecules can be simultaneously assessed for toxicity against a whole organism and efficacy against human cancer cells. Given our findings regarding the effects of temperature on human cell drug response (**Figure 5A-B**) and the static nature of cells when xenografted into yolk (**Figure 6**) we wanted to assess the effects of drug treatment on xenografted T-ALL cells. Metabolic analysis showed that zebrafish larvae treated with Dexamethasone and Vincristine cluster separately from each other and DMSO treated larvae, indicating that these drugs are well-absorbed by larvae as they created global metabolic changes in the animal (**Supplemental Figure 2**). We xenografted GFP-expressing Jurkat cells into the pericardium and yolk of zebrafish larvae at 2 dpf and then subjected them to drug treatment with Dexamethasone or Vincristine starting at 1 dpt at 34°C or 37°C. Jurkat cells are resistant to Dexamethasone but sensitive to Vincristine (**Figure 5A**). TUNEL staining after 48hr of drug treatment showed almost no apoptosis in cells when larvae were maintained at 34°C, whether cells were xenografted into the pericardial space or the yolk (**Figure 7A-D**). At 34°C, two animals examined had a small percentage of TUNEL-positive cells with Vincristine treatment, however these data were not significantly different than DMSO treated cells (**Figure 7A-B**). At 37°C, we observed that cells xenografted into the pericardial space had significantly more apoptosis when treated with Vincristine compared to DMSO (23% TUNEL-positive compared to 0%, respectively, p=0.021**, Figure 7A-B**), and cells were not killed by

Dexamethasone, as expected. We observed some apoptosis in yolk-injected xenografts housed at 37°C, but only in a small number of animals per group and across all treatments (**Figure 7C-7D**).

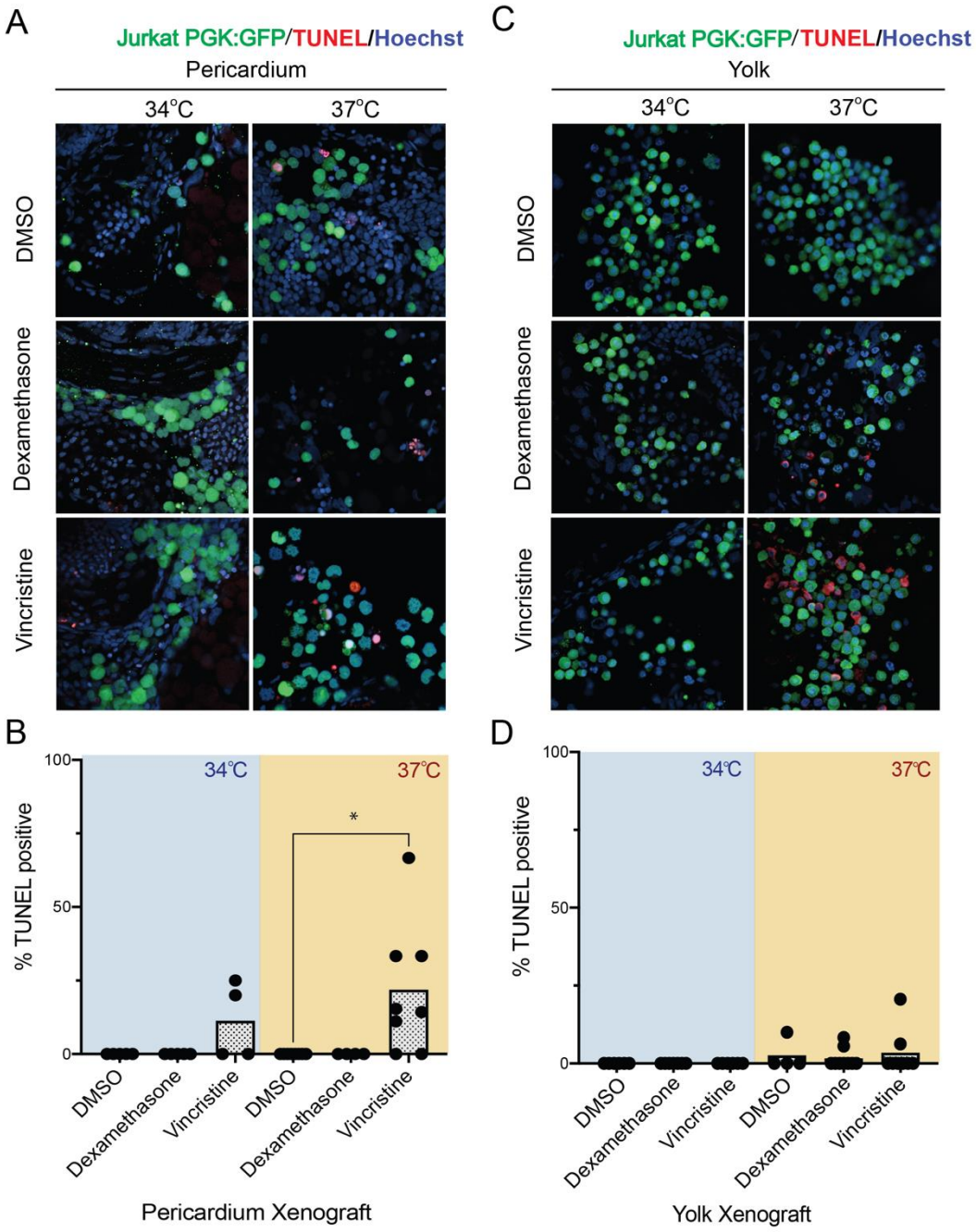

Figure 7. Xenografts in the pericardial space of larvae housed at 37°C produce the most consistent drug response. GFP expressing Jurkat cells were xenografted into the pericardium or yolk of zebrafish larvae and subjected to drug treatment with 10 μM Dexamethasone, 10 μM Vincristine, or DMSO vehicle control for 2 days post-transplant at 34°C or 37°C, as indicated. Jurkat cells are known to be resistant to Dexamethasone, but are sensitive to Vincristine. Drug-treated larvae were fixed and stained with TUNEL to quantify apoptosis in GFP-positive cells. (**A**) Representative TUNEL staining of pericardium transplanted cells. The percent of TUNEL and GFP-positive cells in all images is quantified in (**B**), which each data point representing one animal and bars representing the average within the treatment group. *p<0.05. (**C**) is representative images from yolk xenografted animals, with the percent TUNEL and GFP-positive cells quantified in (**D**). There is no significant difference between any of these treatment groups.

3. Discussion

Zebrafish have many strengths as a model for human cancer. They are inexpensive to use, ideal for *in vivo* imaging, respond in much the same way has humans to chemotherapy and drug treatment, and can provide a high N value in any experiment. Their use in human cancer xenografts in zebrafish is relatively new but they are already making an impact by identifying potentially new anti-cancer drugs and providing new insight into important cancer processes like metastasis and drug resistance. As with all novel applications, certain challenges should be addressed before the assay moves into widespread use. We set out to resolve some of these issues in efforts to help establish a standardized protocol for zebrafish larval xenograft, so that data obtained from these experiments will be more reproducible across laboratories.

We examined 7 different transplant sites and found that the xenograft procedure caused no significant difference in larval survival, even between sites as varied as yolk and brain. However, as many as 50% of xenografted larvae were unable to survive to 5 days post-transplant, the typical length of a drug screening experiment. We cannot rule out that larval death was due to cancer cell expansion, and larval death can be controlled for experimentally with DMSO/vehicle control. This finding does impact the numbers of larvae needed for experiments, and we now routinely xenograft two times the number of animals needed to power our experiment. Additionally, when starting these experiments, we found entire clutches of larvae might die after xenograft or after one day of drug treatment, for no identifiable reason. We now use adult fish between 6 months and one year of age for breeding to provide larvae for xenograft experiments and will no longer xenograft into larva if a clutch does not appear robust. Finally, while the type of cancer cells used in xenograft has no impact on engraftment rate or larva survival, the maximum amount of cells able to be xenografted was less than 1,000. This low number of cells is beneficial in that it will allow for many larvae to be xenografted when tumor sample is limited, such as with a primary patient sample. At the same time, this limits the ability to use zebrafish to expand patient derived samples for cryopreservation, such as is commonly done in mice. Additionally, while concerns that this low cell number would not fully encompass the true extent of intratumoral heterogeneity are valid, they can be somewhat ameliorated by injection of many larvae with the same patient sample. Immunocompromised adult zebrafish can also be xenografted with hundreds of thousands of cells [13,47] —while the adult model is not ideal for high-throughput screening, transplants in adult zebrafish will likely more accurately represent the effects of tumor heterogeneity in an experimental assays.

Our findings that temperature can decrease zebrafish survival and impact human cell proliferation are supported by several other studies [32,36]. We also examined the metabolic basis of these effects by profiling the effects that non-physiologic temperatures had on global metabolism of zebrafish larvae and human cells. As expected, we found significant global metabolic changes in zebrafish as they were moved from their ideal 28°C to 34°C. However, there was no further change in metabolic program as fish moved from 34°C to 37°C. Fish survived very well at high temperatures for 3 days, with their health beginning to precipitously decline after 4 days of housing at warmer temperatures. At this point, we observed the yolk to be nearly consumed—it is likely that higher temperatures increased the larvae's energy consumption beyond what the yolk could provide. It may be possible to counteract this starvation by supplying the larva with an alternate food source, such as paramecia or rotifers. This may provide an additional benefit in drug experiments as these microorganisms may absorb some of the drug and be subsequently consumed by the zebrafish.

We also found an expected change in metabolism, particularly mitochondrial bioenergetics, as human cancer cells were cultured at 34°C, compared to their physiologic 37°C. Unsurprisingly, this

led to some drugs, such as Methotrexate, being ineffective at lower temperatures in some cell lines. Additionally, upon xenograft, while human cells were able to proliferate at 34°C in the zebrafish, their response to chemotherapy was significantly dampened at 34°C, with almost no cells undergoing apoptosis. The same cells were able to respond to drug when larvae were housed at 37°C . Given that some zebrafish larvae do survive at 37°C, and could possibly survive well if given proper nutrition, our data suggest that all xenografts should be carried out at 37°C for a more accurate assessment of human cancer cell response to drug. While many zebrafish xenograft studies have used 34°C as a "compromise" between the physiological needs of zebrafish and human cells, we have found that the overall metabolic effects of warmer temperatures on zebrafish don't profoundly change between 34°C and 37°C, while the metabolic effects of cooler temperatures on human cells at 34°C and 37°C are much more significant.

Finally, we examined the effects of xenograft into the yolk versus the soma of the zebrafish, here the soma was the pericardial space. Not unexpectedly, the metabolites that are available to xenografted cells in the yolk and soma of the zebrafish are different—overall, metabolites are more enriched in the yolk. We were surprised to find that xenografted cells were not proliferating in the yolk. Generally the yolk is considered nutrient-rich, and along with ease of injection, this has made the yolk a common site of xenograft. In our hands, cells xenografted into the yolk did not proliferate, undergo apoptosis, or respond well to drug. The acellular, lipid-rich microenvironment might have been too different from the physiological needs of the cancer cells, and pushed them into a static state. While we tested several cell lines and cancer types, we cannot rule out that other cells or patient derived samples may behave differently upon transplant into zebrafish yolk.

In total, our study examined the cellular and metabolic response of both the zebrafish and human cancer cells to xenograft and provided experimental evidence that temperature and transplant site can affect the results of a zebrafish xenograft assay. We found that, ideally, cells would be xenografted into the soma of the zebrafish and animals housed at 37°C. Housing at lower temperatures does not necessarily benefit the zebrafish larva but does impact how well human cells are able to respond to drug treatment. Importantly, our studies focused exclusively on zebrafish xenograft for large scale drug screening—other xenograft studies, such as examination of cancer cell interactions with the tumor microenvironment, may require zebrafish to be housed closer their physiologic conditions. Ultimately, zebrafish xenograft will not replace the use of mammalian xenograft models, but they are a useful bridge between *in vitro* drug screening and mouse xenograft. In some cases where *in vitro* cell culture is not possible, such as use of patient derived samples, zebrafish provide an excellent opportunity to rapidly test cancer cell response to panels of drugs. Standardized methods for zebrafish xenograft are an important step as this model becomes more commonly used in cancer research and, possibly, as a tool for personalized medicine.

4. Materials and Methods

4.1 Zebrafish care and use

Use and handling of zebrafish was approved by the University of Kentucky's Institutional Animal Care and Use Committee (IACUC), protocol 2019-3399. Casper, AB, and SAT strain zebrafish were used for these studies. Adult zebrafish were maintained at a temperature of 28°C with a light/dark cycle of 14:10 hours in compliance with IACUC animal care regulations. Eggs were collected into 1X E3 media (14.6 g of 5.0 mM NaCl, 0.65 g of 0.17 mM KCl, 2.20 g of 0.33 mM CaCl, and 4.05 g of 0.33 mM $MgSO_4$ per liter of 50X stock) with 200 μL/L of methylene blue.

4.2 Cell culture

All human cell lines were cultured at 37°C in a humidified atmosphere with 5% CO2. Cell lines were authenticated by short tandem repeat (STR) DNA profiling and tested for mycoplasma contamination prior to experimentation. All media was supplemented with 10% heat-inactivated fetal bovine serum (FBS, Atlanta Biologicals, S11150H, Lot M17161). Human T-cell acute lymphoblastic leukemia (T-ALL) cell lines, including Jurkat (ATCC, TIB-152), HSB2 (ATCC, CCL-120.1), and HPB-ALL (DSMZ, ACC 483) cells were grown in RPMI 1640 (ThermoFisher 11875119). GFP-labeled Jurkat, HSB2, and HPB-ALL cells were generated using a pLENTI-PGK:GFP expression construct as previously described [48]. DLD-1 colon cancer cells (ATCC, CCL-221) were cultured in RPMI 1640 media. Daoy medulloblastoma cells (ATCC, HTB-186) were cultured in EMEM (ATCC, 30-2003). Murine-derived lung cancer cell lines UK777 and UK657 were a generous gift from Dr. Christine Brainson, University of Kentucky, and were cultured in DMEM/F12 (Thermo Fisher Scientific, 10565018), supplemented with 1% Glutamax (Fisher Scientific, 35-050-061), and 1% Insulin Transferrin Selenium (Fisher Scientific, 41-400-045). Breast cancer cell lines MCF-7 (ATCC, CRL-3435) and MDA-MB-231 (ATCC, CRM-HTB-26) were cultured in DMEM (Life Technologies, 11965118) and DMEM/F12, respectively.

To assess the effects of temperature change on metabolic profiles, cells at 60% confluency were incubated at either 28°C, 34°C, or 37°C in a humidified atmosphere with 5% CO2 for 24 hours before samples were prepared for mass spectrometry analysis.

For cell growth assays, cells were counted on a Vi-Cell XR cell viability analyzer (Beckman Coulter) and 50,000 cells were plated per well of a 12 well plate in triplicate wells. Cells were incubated at either 28°C, 34°C, or 37°C in a humidified atmosphere with 5% CO2. Viable cells were counted on the Vi-Cell XR cell viability analyzer at days 1, 3 and 5 after plating.

To determine IC_{50} of chemotherapy treatment for T-ALL cells at 37°C and 34°C, 50 µL of HBP-ALL or HSB2 (both at 2×10^5 cells/ml) or Jurkat (1×10^5 cells/mL) cells were plated in triplicate wells. Cytarabine (Selleck, S1648), Dexamethasone (VWR, 89157-624), Methotrexate (Sigma-Aldrich, A6770), and Vincristine (Selleck, S1241), and DMSO were diluted to 2X the desired concentration in cell culture media, and then 50 µL were added to the well. Then the cells were cultured at 37°C or 34°C in a humidified atmosphere with 5% CO2 for 72 hours. CellTiter-Glo Luminescent Cell Viability Assay (Promega, G7570) was used to measure cell survival according to the manufacturer's instructions. A Synergy LX BioTek multi-mode plate reader was used to read luminescent signal.

To compare apoptosis of T-ALL cells at 37°C and 34°C, 500 µL of HPB-ALL or HSB2 (1×10^5 cells/ml) or Jurkat (5×10^4 cells/mL) cells were seeded in the 24-well cell culture plate and then cultured at 37°C or 34°C in a humidified atmosphere with 5% CO2 for 72 hours. The cells were harvested and apoptosis was quantified by staining cells with Annexin V APC (ThermoFisher 88-8007-74) according to the manufacturers protocol, in the presence of DAPI (0.05 µg/ml). Staining was quantified via flow cytometry.

4.3 Xenograft of human cells into zebrafish

Prior to cell staining, viable Jurkat, HSB2, or HPB-ALL cells were counted using a Countess® Automated Cell Counter system (Invitrogen, C10227). Cells were stained immediately prior to injection using Vybrant DiI Cell-Labeling Solution (Invitrogen, V22885). DiI was diluted to a final concentration of 4 µg/mL in 5 mL room-temperature, 1X phosphate-buffered saline (PBS, Caisson Labs, PBL06-6X500ML). Cells were centrifuged at 1200 rpm for 5minutes, resuspended in the 5 mL DiI + 1X PBS solution, incubated at 37°C for 10 minutes in the dark, then washed 3x using 5 mL of a RPMI + 10% FBS solution that was pre-warmed to 37°C, with centrifugation at 1200 rpm for 5 minutes for each wash. Cells were filtered through a sterile 40µm cell strainer to ensure a single cell suspension. Finally, the stained cells were resuspended in the pre-warmed RPMI + 10% FBS

solution to a concentration that would deliver 500 cells in a 2 nL injection volume. For cell number studies, cells were resuspended at varying concentrations to deliver 100, 250, 500, or 1,000 cells per 2 nL injection volume.

Zebrafish larvae at 48 hours post-fertilization (hpf) were dechorionated with Pronase (Fisher Scientific, 74-332) at a final concentration of 1mg/mL in 1xE3 media, immediately prior to xenograft. Transplants of human cells into zebrafish were performed using non-filament borosilicate glass capillaries (Sutter Instrument Company, B100-50-10). Capillaries were heated and pulled into needlepoints using a Flaming/Brown micropipette puller (Sutter Instrument, P-87). Needlepoints were cut to a bevel using a sterile razor. Droplet size was measured to 2 nL (~0.15mm diameter) using a micrometer and kept at a constant volume throughout injection. Two-day post-fertilization (dpf) larave were anesthetized prior to microinjection using 4 mg/mL Tricaine-S (Pentair Aquatic, NC0342409). Xenograft injections were performed using an air-pressure driven system (MPPI-3 Pressure Injector and Microinjector Pipette Holder, ASI). Post-injection, embryos were kept in 1X E3 media and incubated at 28°C for a 1-hour recovery time then moved to either 34°C or 37°C. If clumping of cells in the micropipette occurred, needles were chilled on ice prior to loading with cells.

Embryos were screened at 24, 72, and 120 hours post-transplant (hpt) for survival studies. Initial screening for cancer cell engraftment was performed using a Nikon SMZ18 fluorescence microscope. Dead embryos and embryos without engrafted cancer cells were removed at 24 hpt.

4.4 Zebrafish immunofluorescence and imaging experiments

For TUNEL staining, embryos were fixed in 4% PFA overnight followed by graded methanol dehydration. Fixed embryos were rehydrated with PBS and permeabilized in 0.1% Sodium Citrate, 0.1% TritonX, 20 µg/ml Proteinase K for 30 min at room temperature then washed extensively in PBS. TUNEL solution was mixed as per manufacturer's instructions using either the TMR or Fluorescien kit (Sigma-Aldrich 11684795910 and 12156792910) and added to embryos for 1hr in the dark, followed by five PBS washes and staining with 1:1000 Hoechst 33342 (ThermoFisher H3570).

For BrdU staining, larvae were treated with 10 mM BrdU for 24 hrs post-transplant, followed by fixation in 4% PFA and graded methanol dehydration. After rehydrating with PBS, tissues were permeabilized in 20 µg/ml Proteinase K solution for 1 hr and denatured in 2N HCl for 1 hr. Blocking was done in 2% BSA. Larvae were stained with anti-BrdU (BD cat#A11001) at 1:200 with a mixture of 1:1000 Hoechst stain.

All imaging was carried out on a Nikon A1 inverted confocal using NIS Elements software. Larvae were mounted and cover slipped on glass slides in 3% Methylcellulose. All exposure settings were first adjusted to negative controls.

4.5 Xenograft drug treatment

Xenografted larvae that were injected with either Jurkat or HSB2 cells were screened for consistent cell engraftment then treated with DMSO, Dexamethasone, or Vincristine at a 10uM concentration in E3 media. Experiments were carried out as previously described [20] and animals were collected for TUNEL staining as described above.

4.6 Sample preparation for metabolism experiments

To examine the effect of temperature on zebrafish metabolism, zebrafish were manually dechorionated at 2 dpf and placed at either 28°C, 34°C, or 37°C with 30 embryos per 10 cm^2 dish in E3 media for 24 hours. After 24 hours, zebrafish were sacrificed by rapid chilling on ice, and processed for Mass Spectrometry (MS) analysis as described below. To examine drug metabolism in

zebrafish, 4 dpf larvae were treated with either 25 μM vincristine or 10 μM dexamethasone in E3 media in 10 cm^2 dishes with 30 embryos per dish for 48 hours at 34°C or 37°C. Zebrafish larvae were sacrificed by rapid chilling on ice and processed for MS analysis as described below. For all MS experiments, a total of ~100 mg of tissue was needed for metabolomic analysis, which required about 120 zebrafish larvae per sample, with each sample done in triplicate.

Euthanized zebrafish larvae were collected into 1.5 mL tubes, the E3 media was removed, and fish were washed with 1 mL of ice-cold 0.9X PBS + 4% BSA. To de-yolk zebrafish, fish were pipetted up and down with a P200 pipette tip approximately 20 times in 200 μL of ice-cold 0.9X PBS + 4% BSA until yolks were removed. The supernatant was then removed and de-yolked fish were washed 2 more times with 1 mL of ice-cold 0.9X PBS + 4% BSA. A quick spin (~5 sec) in a benchtop microcentrifuge was done to pellet larvae, all supernatant was removed, cotton swab to dry the inside of the tube. Samples were flash frozen in liquid nitrogen.

Zebrafish pellets were removed from cryostorage and transferred to a mircovial set (6757) for use with a Freezer/Mill Cryogenic Grinder (SPEX SamplePrep model 6875D). Fish were pulverized to 5 μm particles. Metabolites were extracted directly from the microvial by the addition of 1 ml of 50% methanol containing 20 M L-norvaline (procedural, internal control) and separated into polar (aqueous layer) and insoluble pellet (protein/DNA/RNA/glycogen) by centrifugation at 4°C, 15,000rpm for 10 minutes. The pellet was subsequently washed four times with 50% methanol and once with 100% methanol to remove polar contaminants. The polar fraction was dried at 10-3 mBar using a SpeedVac (Thermo) followed by derivatization. The insoluble pellet was hydrolyzed as previously described [49].

4.7 Sample derivatization and Gas Chromatography-Mass Spectrometry (GC-MS) quantitation

Dried polar and insoluble samples were derivatized by the addition of 20 mg/ml methoxyamine hydrochloride in pyridine and incubated for 1.5 hrs at 30°C. Sequential addition of N-methyl-trimethylsilyl-trifluoroacetamide (MSTFA) followed with an incubation time of 30 minutes at 37°C with thorough mixing between addition of solvents. The mixture was then transferred to a v-shaped amber glass chromatography vial and analyzed by GC-MS.

An Agilent 7800B gas-chromatography coupled to a 5977B mass spectrometry (GCMS) detector was used for this study. GC-MS protocols were similar to those described previously [50,51], except a modified temperature gradient was used for GC: Initial temperature was 130°C, held for 4 minutes, rising at 6°C/minutes to 243°C, rising at 60°C/minutes to 280°C, held for 2 minutes. The electron ionization (EI) energy was set to 70 eV. Scan (m/z:50-800) and full scan mode were used for metabolomics analysis. Mass spectra were translated to relative metabolite abundance using the Automated Mass Spectral Deconvolution and Identification System (AMDIS) software matched to the FiehnLib metabolomics library (available through Agilent) [51]. Quantitation was performed using the software Data Extraction for Stable Isotope-labelled metabolites (DExSI) [52]. Relative abundance was corrected for recovery using the L-norvaline standard and adjusted to protein input.

4.8 Seahorse metabolism experiments

Cells were cultured overnight at 34°C or 37°C in a humidified atmosphere with 5% CO_2. A Seahorse Xfe96 PDL Miniplate was coated fresh with Cell-Tak Cell and Tissue Adhesive (Corning, 354240) at a dilution factor of 79.5 in 0.1M sodium bicarbonate and washed twice with distilled water. The coating and wash processes were repeated a second time. Cells were then plated at a cell density of 70,000 cells/well for Jurkat cells or 100,000 cells/well for HSB2 cells in RPMI 1640 supplemented with 10% heat-inactivated FBS, allowed to incubate for 5 minutes at room

temperature, and spun down at 200xg for 1 minute with zero brake. The plate was then incubated at 34°C or 37°C for 30 mins before media was replaced with assay media (below).

All OCR and ECAR analyses were performed with a minimum of 6–8 technical replicates for each treatment or assay. All cells were incubated for 60 min in a non-CO2 incubator before plate calibration was performed and mitochondria and glycolytic rate test experiments were initiated at corresponding temperature conditions.

The Seahorse XFe96 (Agilent Technologies) was used to measure oxygen consumption rates (OCR) or extracellular acidification rates (ECAR) of cells. One hour prior to assay, growth media was replaced with XF RPMI assay media supplemented with 2 mM L-glutamine, 1 mM pyruvate, and 10 mM glucose (assay media and all supplements from Agilent Technologies). Cells were then placed in the non-CO_2, 34°C or 37°C Bio-tek Cytation 1 for degassing and brightfield image scanning. The Seahorse XFe96 sensor cartridge was calibrated, and the degassed microplate was then placed in the Seahorse XFe96. For mitochondrial stress assays baseline OCR and ECAR measurements were followed by acute injections of oligomycin (1uM), FCCP (0.6uM), and a combination of antimycin A (1uM) and rotenone (1uM). For glycolytic rate assays baseline PER measurements were followed by acute injections of a combination of antimycin A (1uM) and rotenone (1uM) followed by 50mM 2DG. The Seahorse data was viewed with Wave 2.6.0.

4.9 Statistical analysis

Statistical analyses were carried out using GraphPad Prism. One-way ANOVA with Tukey's test for comparison of means was used for comparison of day 5 values of % survival and cell growth studies. All metabolic numerical data are presented as mean ± Standard Error (SE). A P-value less than 0.05 using a student t-test was considered statistically significant. Clustering heatmap and partial least squares discriminant analysis (PLS-DA) were performed using the MetaboAnalyst package for R (available through MetaboAnalyst, https://www.metaboanalyst.ca/) [53,54]. For PLS-DA and heatmap analysis log-transformed metabolomics data were used, and unit variance scaling was employed for row numbers and SVD with imputation for PLS-DA clustering. Correlation and tightest cluster first options were used for heatmap visualization [53,54]. All available metabolomics data points were used for multivariant analysis.

5. Conclusions

Zebrafish xenografts are undoubtedly an important complement to mouse xenograft models, and they may have an exciting future in personalized cancer medicine. We have found that variations in xenograft transplant site and animal housing temperature can result in widely different effects on the cellular and metabolic responses of both human cells and recipient zebrafish. Our data suggest that when zebrafish xenografts are to be used for drug screening purposes, transplant of cells into the soma, not the yolk, and housing at 37°C are likely to provide the most accurate drug response results. Standardized methods for zebrafish xenografts will allow this model to be more widely used in cancer research.

Supplementary Materials: The following are available online at www.mdpi.com/xxx/s1
Figure S1. Apoptosis and proliferation rates of cells stained with DiI
Figure S2. Chemotherapy treatments cause metabolic shifts in zebrafish larvae
Table S1. Larvae survival and engraftment vary between injection sites
Table S2. Survival of xenografted larvae varies with different rearing temperatures
Table S3. Metabolites present in zebrafish larvae vary at different rearing temperatures
Table S4. Metabolite composition of Jurkat cells grown at 34°C and 37°C
Table S5. Metabolite composition varies across whole body and yolk depleted tissue

Author Contributions: Conceptualization, M.H. and J.B.; methodology, M.H., J.B., and R.S.; investigation, M.H., L.Y., L.M., S.D., Y.C., M.W, and W.S.; formal analysis, M.H., L.Y., Y.C., K.M., and A.P.; resources, J.S.B. and

R.C.S.; writing—original draft preparation, M.H.; writing—review and editing, J.B. and R.S.; supervision and funding acquisition, J.B. and R.S. All authors have read and agreed to the published version of the manuscript.

Funding: This research was funded by NIH Training Grant T32CA165990 (M.G.H.), NIH DP2CA228043 and the Kentucky Pediatric Cancer Research Trust (J.S.B.) and R01AG066653, the St. Baldrick's Career Development Award, the V-Scholar Grant and the Rally Foundation Independent Investigator Grant (R.C.S) Research reported in this publication was also supported by the Redox Metabolism and Flow Cytometry and Immune Monitoring Shared Resource(s) of the University of Kentucky Markey Cancer Center (P30CA177558) and by the Office of the Director of the National Institutes of Health under Award Number S10OD025033.

Acknowledgments: We would like to thank Drs. Kathleen O'Conner, Tianyan Gao, and Cristene Brainson for providing some of the cell lines used in this study. We are grateful to Dr. Tomoko Sengoku for her assistance in optimization of Seahorse experiments and support in data analysis. Thank you to Caroline Smith, Shilpa Sampathi, Trace Jolly, and Viral Oza for helpful feedback during the manuscript editing process. Biorender.com was used for the graphical abstract and schematics.

Conflicts of Interest: The authors declare no conflict of interest.

References

1. Brown, H.K.; Schiavone, K.; Tazzyman, S.; Heymann, D.; Chico, T.J. Zebrafish xenograft models of cancer and metastasis for drug discovery. *Expert Opin Drug Discov* **2017**, *12*, 379-389, doi:10.1080/17460441.2017.1297416.
2. Chen, X.; Li, Y.; Yao, T.; Jia, R. Benefits of Zebrafish Xenograft Models in Cancer Research. *Front Cell Dev Biol* **2021**, *9*, 616551, doi:10.3389/fcell.2021.616551.
3. Fazio, M.; Ablain, J.; Chuan, Y.; Langenau, D.M.; Zon, L.I. Zebrafish patient avatars in cancer biology and precision cancer therapy. *Nat Rev Cancer* **2020**, *20*, 263-273, doi:10.1038/s41568-020-0252-3.
4. Zon, L.I.; Peterson, R.T. In vivo drug discovery in the zebrafish. *Nat Rev Drug Discov* **2005**, *4*, 35-44, doi:10.1038/nrd1606.
5. Stoletov, K.; Klemke, R. Catch of the day: zebrafish as a human cancer model. *Oncogene* **2008**, *27*, 4509-4520, doi:10.1038/onc.2008.95.
6. Astone, M.; Dankert, E.N.; Alam, S.K.; Hoeppner, L.H. Fishing for cures: The alLURE of using zebrafish to develop precision oncology therapies. *NPJ Precis Oncol* **2017**, *1*, doi:10.1038/s41698-017-0043-9.
7. Cornet, C.; Dyballa, S.; Terriente, J.; Di Giacomo, V. ZeOncoTest: Refining and Automating the Zebrafish Xenograft Model for Drug Discovery in Cancer. *Pharmaceuticals (Basel)* **2019**, *13*, doi:10.3390/ph13010001.
8. Rennekamp, A.J.; Peterson, R.T. 15 years of zebrafish chemical screening. *Curr Opin Chem Biol* **2015**, *24*, 58-70, doi:10.1016/j.cbpa.2014.10.025.
9. White, R.M.; Sessa, A.; Burke, C.; Bowman, T.; LeBlanc, J.; Ceol, C.; Bourque, C.; Dovey, M.; Goessling, W.; Burns, C.E.; et al. Transparent adult zebrafish as a tool for in vivo transplantation analysis. *Cell Stem Cell* **2008**, *2*, 183-189, doi:10.1016/j.stem.2007.11.002 10.1016/j.stem.2007.11.002.
10. Lam, S.H.; Chua, H.L.; Gong, Z.; Lam, T.J.; Sin, Y.M. Development and maturation of the immune system in zebrafish, Danio rerio: a gene expression profiling, in situ hybridization and immunological study. *Dev Comp Immunol* **2004**, *28*, 9-28, doi:10.1016/s0145-305x(03)00103-4.

11. Lee, L.M.; Seftor, E.A.; Bonde, G.; Cornell, R.A.; Hendrix, M.J. The fate of human malignant melanoma cells transplanted into zebrafish embryos: assessment of migration and cell division in the absence of tumor formation. *Dev Dyn* **2005**, *233*, 1560-1570, doi:10.1002/dvdy.20471.
12. Topczewska, J.M.; Postovit, L.M.; Margaryan, N.V.; Sam, A.; Hess, A.R.; Wheaton, W.W.; Nickoloff, B.J.; Topczewski, J.; Hendrix, M.J. Embryonic and tumorigenic pathways converge via Nodal signaling: role in melanoma aggressiveness. *Nat Med* **2006**, *12*, 925-932, doi:10.1038/nm1448.
13. Yan, C.; Brunson, D.C.; Tang, Q.; Do, D.; Iftimia, N.A.; Moore, J.C.; Hayes, M.N.; Welker, A.M.; Garcia, E.G.; Dubash, T.D.; et al. Visualizing Engrafted Human Cancer and Therapy Responses in Immunodeficient Zebrafish. *Cell* **2019**, *177*, 1903-1914.e1914, doi:10.1016/j.cell.2019.04.004.
14. Costa, B.; Estrada, M.F.; Mendes, R.V.; Fior, R. Zebrafish Avatars towards Personalized Medicine-A Comparative Review between Avatar Models. *Cells* **2020**, *9*, doi:10.3390/cells9020293.
15. Rajan, V.; Melong, N.; Hing Wong, W.; King, B.; Tong, S.R.; Mahajan, N.; Gaston, D.; Lund, T.; Rittenberg, D.; Dellaire, G.; et al. Humanized zebrafish enhance human hematopoietic stem cell survival and promote acute myeloid leukemia clonal diversity. *Haematologica* **2020**, *105*, 2391-2399, doi:10.3324/haematol.2019.223040.
16. Corkery, D.P.; Dellaire, G.; Berman, J.N. Leukaemia xenotransplantation in zebrafish--chemotherapy response assay in vivo. *Br J Haematol* **2011**, *153*, 786-789, doi:10.1111/j.1365-2141.2011.08661.x.
17. Deveau, A.P.; Bentley, V.L.; Berman, J.N. Using zebrafish models of leukemia to streamline drug screening and discovery. *Exp Hematol* **2017**, *45*, 1-9, doi:10.1016/j.exphem.2016.09.012.
18. Pardo-Martin, C.; Chang, T.Y.; Koo, B.K.; Gilleland, C.L.; Wasserman, S.C.; Yanik, M.F. High-throughput in vivo vertebrate screening. *Nat Methods* **2010**, *7*, 634-636, doi:10.1038/nmeth.1481.
19. Chang, T.Y.; Pardo-Martin, C.; Allalou, A.; Wählby, C.; Yanik, M.F. Fully automated cellular-resolution vertebrate screening platform with parallel animal processing. *Lab Chip* **2012**, *12*, 711-716, doi:10.1039/c1lc20849g.
20. Haney, M.G.; Moore, L.H.; Blackburn, J.S. Drug Screening of Primary Patient Derived Tumor Xenografts in Zebrafish. *J Vis Exp* **2020**, doi:10.3791/60996.
21. Ghotra, V.P.; He, S.; de Bont, H.; van der Ent, W.; Spaink, H.P.; van de Water, B.; Snaar-Jagalska, B.E.; Danen, E.H. Automated whole animal bio-imaging assay for human cancer dissemination. *PLoS One* **2012**, *7*, e31281, doi:10.1371/journal.pone.0031281.
22. Zhang, F.; Qin, W.; Zhang, J.P.; Hu, C.Q. Antibiotic toxicity and absorption in zebrafish using liquid chromatography-tandem mass spectrometry. *PLoS One* **2015**, *10*, e0124805, doi:10.1371/journal.pone.0124805.
23. Morikane, D.; Zang, L.; Nishimura, N. Evaluation of the Percutaneous Absorption of Drug Molecules in Zebrafish. *Molecules* **2020**, *25*, doi:10.3390/molecules25173974.
24. Cassar, S.; Adatto, I.; Freeman, J.L.; Gamse, J.T.; Iturria, I.; Lawrence, C.; Muriana, A.; Peterson, R.T.; Van Cruchten, S.; Zon, L.I. Use of Zebrafish in Drug Discovery Toxicology. *Chem Res Toxicol* **2020**, *33*, 95-118, doi:10.1021/acs.chemrestox.9b00335.
25. Nicoli, S.; Presta, M. The zebrafish/tumor xenograft angiogenesis assay. *Nat Protoc* **2007**, *2*, 2918-2923, doi:10.1038/nprot.2007.412.
26. Haldi, M.; Ton, C.; Seng, W.L.; McGrath, P. Human melanoma cells transplanted into zebrafish proliferate, migrate, produce melanin, form masses and stimulate angiogenesis in zebrafish. *Angiogenesis* **2006**, *9*, 139-151, doi:10.1007/s10456-006-9040-2.

27. Veinotte, C.J.; Dellaire, G.; Berman, J.N. Hooking the big one: the potential of zebrafish xenotransplantation to reform cancer drug screening in the genomic era. *Dis Model Mech* **2014**, *7*, 745-754, doi:10.1242/dmm.015784.
28. Fraher, D.; Sanigorski, A.; Mellett, N.A.; Meikle, P.J.; Sinclair, A.J.; Gibert, Y. Zebrafish Embryonic Lipidomic Analysis Reveals that the Yolk Cell Is Metabolically Active in Processing Lipid. *Cell Rep* **2016**, *14*, 1317-1329, doi:10.1016/j.celrep.2016.01.016.
29. Mercatali, L.; La Manna, F.; Groenewoud, A.; Casadei, R.; Recine, F.; Miserocchi, G.; Pieri, F.; Liverani, C.; Bongiovanni, A.; Spadazzi, C.; et al. Development of a Patient-Derived Xenograft (PDX) of Breast Cancer Bone Metastasis in a Zebrafish Model. *Int J Mol Sci* **2016**, *17*, doi:10.3390/ijms17081375.
30. Hill, D.; Chen, L.; Snaar-Jagalska, E.; Chaudhry, B. Embryonic zebrafish xenograft assay of human cancer metastasis. *F1000Res* **2018**, *7*, 1682, doi:10.12688/f1000research.16659.2.
31. Drabsch, Y.; Snaar-Jagalska, B.E.; Ten Dijke, P. Fish tales: The use of zebrafish xenograft human cancer cell models. *Histol Histopathol* **2017**, *32*, 673-686, doi:10.14670/hh-11-853.
32. Cabezas-Sainz, P.; Guerra-Varela, J.; Carreira, M.J.; Mariscal, J.; Roel, M.; Rubiolo, J.A.; Sciara, A.A.; Abal, M.; Botana, L.M.; López, R.; et al. Improving zebrafish embryo xenotransplantation conditions by increasing incubation temperature and establishing a proliferation index with ZFtool. *BMC Cancer* **2018**, *18*, 3, doi:10.1186/s12885-017-3919-8.
33. Cabezas-Sáinz, P.; Pensado-López, A.; Sáinz, B., Jr.; Sánchez, L. Modeling Cancer Using Zebrafish Xenografts: Drawbacks for Mimicking the Human Microenvironment. *Cells* **2020**, *9*, doi:10.3390/cells9091978.
34. Vergauwen, L.; Benoot, D.; Blust, R.; Knapen, D. Long-term warm or cold acclimation elicits a specific transcriptional response and affects energy metabolism in zebrafish. *Comp Biochem Physiol A Mol Integr Physiol* **2010**, *157*, 149-157, doi:10.1016/j.cbpa.2010.06.160.
35. Vergauwen, L.; Knapen, D.; Hagenaars, A.; Blust, R. Hypothermal and hyperthermal acclimation differentially modulate cadmium accumulation and toxicity in the zebrafish. *Chemosphere* **2013**, *91*, 521-529, doi:10.1016/j.chemosphere.2012.12.028.
36. Schnurr, M.E.; Yin, Y.; Scott, G.R. Temperature during embryonic development has persistent effects on metabolic enzymes in the muscle of zebrafish. *J Exp Biol* **2014**, *217*, 1370-1380, doi:10.1242/jeb.094037.
37. Pype, C.; Verbueken, E.; Saad, M.A.; Casteleyn, C.R.; Van Ginneken, C.J.; Knapen, D.; Van Cruchten, S.J. Incubation at 32.5°C and above causes malformations in the zebrafish embryo. *Reprod Toxicol* **2015**, *56*, 56-63, doi:10.1016/j.reprotox.2015.05.006.
38. Vergauwen, L.; Knapen, D.; Hagenaars, A.; De Boeck, G.; Blust, R. Assessing the impact of thermal acclimation on physiological condition in the zebrafish model. *J Comp Physiol B* **2013**, *183*, 109-121, doi:10.1007/s00360-012-0691-6.
39. Hotamisligil, G.S.; Davis, R.J. Cell Signaling and Stress Responses. *Cold Spring Harb Perspect Biol* **2016**, *8*, doi:10.1101/cshperspect.a006072.
40. Schröder, M.; Kaufman, R.J. The mammalian unfolded protein response. *Annu Rev Biochem* **2005**, *74*, 739-789, doi:10.1146/annurev.biochem.73.011303.074134.
41. Boutilier, R.G. Mechanisms of cell survival in hypoxia and hypothermia. *J Exp Biol* **2001**, *204*, 3171-3181.
42. Zaal, E.A.; Berkers, C.R. The Influence of Metabolism on Drug Response in Cancer. *Front Oncol* **2018**, *8*, 500, doi:10.3389/fonc.2018.00500.

43. Chen, X.; Chen, S.; Yu, D. Metabolic Reprogramming of Chemoresistant Cancer Cells and the Potential Significance of Metabolic Regulation in the Reversal of Cancer Chemoresistance. *Metabolites* **2020**, *10*, doi:10.3390/metabo10070289.
44. Beesley, A.H.; Palmer, M.L.; Ford, J.; Weller, R.E.; Cummings, A.J.; Freitas, J.R.; Firth, M.J.; Perera, K.U.; de Klerk, N.H.; Kees, U.R. Authenticity and drug resistance in a panel of acute lymphoblastic leukaemia cell lines. *Br J Cancer* **2006**, *95*, 1537-1544, doi:10.1038/sj.bjc.6603447.
45. Gamble, J.T.; Elson, D.J.; Greenwood, J.A.; Tanguay, R.L.; Kolluri, S.K. The Zebrafish Xenograft Models for Investigating Cancer and Cancer Therapeutics. *Biology (Basel)* **2021**, *10*, doi:10.3390/biology10040252.
46. Sant, K.E.; Timme-Laragy, A.R. Zebrafish as a Model for Toxicological Perturbation of Yolk and Nutrition in the Early Embryo. *Curr Environ Health Rep* **2018**, *5*, 125-133, doi:10.1007/s40572-018-0183-2.
47. Tang, Q.; Abdelfattah, N.S.; Blackburn, J.S.; Moore, J.C.; Martinez, S.A.; Moore, F.E.; Lobbardi, R.; Tenente, I.M.; Ignatius, M.S.; Berman, J.N.; et al. Optimized cell transplantation using adult rag2 mutant zebrafish. *Nat Methods* **2014**, *11*, 821-824, doi:10.1038/nmeth.3031.
48. Wei, M.; Haney, M.G.; Rivas, D.R.; Blackburn, J.S. Protein tyrosine phosphatase 4A3 (PTP4A3/PRL-3) drives migration and progression of T-cell acute lymphoblastic leukemia in vitro and in vivo. *Oncogenesis* **2020**, *9*, 6, doi:10.1038/s41389-020-0192-5.
49. Andres, D.A.; Young, L.E.A.; Veeranki, S.; Hawkinson, T.R.; Levitan, B.M.; He, D.; Wang, C.; Satin, J.; Sun, R.C. Improved workflow for mass spectrometry-based metabolomics analysis of the heart. *J Biol Chem* **2020**, *295*, 2676-2686, doi:10.1074/jbc.RA119.011081.
50. Brewer, M.K.; Uittenbogaard, A.; Austin, G.L.; Segvich, D.M.; DePaoli-Roach, A.; Roach, P.J.; McCarthy, J.J.; Simmons, Z.R.; Brandon, J.A.; Zhou, Z.; et al. Targeting Pathogenic Lafora Bodies in Lafora Disease Using an Antibody-Enzyme Fusion. *Cell Metab* **2019**, *30*, 689-705.e686, doi:10.1016/j.cmet.2019.07.002.
51. Sun, R.C.; Dukhande, V.V.; Zhou, Z.; Young, L.E.A.; Emanuelle, S.; Brainson, C.F.; Gentry, M.S. Nuclear Glycogenolysis Modulates Histone Acetylation in Human Non-Small Cell Lung Cancers. *Cell Metab* **2019**, *30*, 903-916.e907, doi:10.1016/j.cmet.2019.08.014.
52. Dagley, M.J.; McConville, M.J. DExSI: a new tool for the rapid quantitation of 13C-labelled metabolites detected by GC-MS. *Bioinformatics* **2018**, *34*, 1957-1958, doi:10.1093/bioinformatics/bty025.
53. Xia, J.; Psychogios, N.; Young, N.; Wishart, D.S. MetaboAnalyst: a web server for metabolomic data analysis and interpretation. *Nucleic Acids Research* **2009**, *37*, W652-W660, doi:10.1093/nar/gkp356.
54. Pang, Z.; Chong, J.; Li, S.; Xia, J. MetaboAnalystR 3.0: Toward an Optimized Workflow for Global Metabolomics. *Metabolites* **2020**, *10*, doi:10.3390/metabo10050186.